

## Article

# Techno–Econo–Enviro Energy Analysis, Ranking and Optimization of Various Building-Integrated Photovoltaic (BIPV) Types in Different Climatic Regions of Iran

Mehdi Jahangiri <sup>1</sup>, Yasaman Yousefi <sup>2,\*</sup>, Iman Pishkar <sup>3</sup>, Seyyed Jalaladdin Hosseini Dehshiri <sup>4</sup>,  
Seyyed Shahabaddin Hosseini Dehshiri <sup>5</sup> and Seyyed Mohammad Fatemi Vanani <sup>6</sup>

<sup>1</sup> Energy Research Center, Shahrekord Branch, Islamic Azad University, Shahrekord P.O. Box 88137-33395, Iran

<sup>2</sup> Department of Architecture Engineering, Shahrekord Branch, Islamic Azad University, Shahrekord P.O. Box 88137-33395, Iran

<sup>3</sup> Department of Mechanical Engineering, Payame Noor University (PNU), Tehran P.O. Box 19395-4697, Iran

<sup>4</sup> Department of Industrial Management, Faculty of Management and Accounting, Allameh Tabataba'i University, Tehran P.O. Box 14348-63111, Iran

<sup>5</sup> Department of Mechanical Engineering, Sharif University of Technology, Tehran P.O. Box 14588-89694, Iran

<sup>6</sup> Young Researchers and Elite Club, Shahrekord Branch, Islamic Azad University, Shahrekord P.O. Box 88137-33395, Iran

\* Correspondence: y.yousefi@std.iaushk.ac.ir

**Abstract:** Iran is one of the most energy-consuming countries, especially in the construction sector, and more than 40% of its energy consumption is in the construction sector. Therefore, considering the very high potential of Iran in the field of solar energy, the need to pay attention to providing part of the energy required by buildings by solar energy seems necessary. The study of the effect of climate on the performance of a BIPV has not been done in Iran so far. Also, the use of ranking methods using the weighting of parameters affecting the performance of BIPV has not been done so far. The purpose of this study is to investigate the power supply of BIPV connected to the grid in the eight climates of Iran. Technical–economic–environmental energy analyses were performed by HOMER 2.81 software. In order to study different types of BIPV, four angles of 0°, 30°, 60°, and 90° were considered for the installation of solar cells. The effective output parameters of HOMER software were weighted by the Stepwise Weight Assessment Ratio Analysis (SWARA) method based on the opinion of experts, and it was observed that payback time (year) has the highest weight among the studied criteria. Then, different cities were ranked using the evaluation based on distance from the average solution (EDAS) method. The results showed that Jask is the most suitable and Ramsar is the most unsuitable city. Also, the results of the EDAS method were confirmed by Additive Ratio Assessment (ARAS), Weighted Aggregates Sum Product Assessment (WASPAS), and Technique for Order Preference by Similarity to Ideal Solution (TOPSIS) methods.

**Keywords:** HOMER software; simulation; optimization; ranking analysis; BIPV



**Citation:** Jahangiri, M.; Yousefi, Y.; Pishkar, I.; Hosseini Dehshiri, S.J.; Hosseini Dehshiri, S.S.; Fatemi Vanani, S.M. Techno–Econo–Enviro Energy Analysis, Ranking and Optimization of Various Building-Integrated Photovoltaic (BIPV) Types in Different Climatic Regions of Iran. *Energies* **2023**, *16*, 546. <https://doi.org/10.3390/en16010546>

Academic Editors: Jean-Michel Nunzi and Alban Kuriqi

Received: 31 October 2022

Revised: 16 December 2022

Accepted: 21 December 2022

Published: 3 January 2023



**Copyright:** © 2023 by the authors. Licensee MDPI, Basel, Switzerland. This article is an open access article distributed under the terms and conditions of the Creative Commons Attribution (CC BY) license (<https://creativecommons.org/licenses/by/4.0/>).

## 1. Introduction

Despite the technical maturity and significant cost reduction of BIPV technology, this technology is still associated with challenges to expanding its applications and universality [1]. One of these challenges is to examine the degree of adaptation of BIPVs to different weather conditions in a country so that the decision-makers in this area can make better decisions regarding the development of BIPVs and the reduction of climate change [2]. Other important points in front of researchers and decision-makers are finding the optimal configuration for placing solar cells on the facade of the building (finding the best type of BIPV) and also weighting the effective parameters in the problem in order to rank different stations. The mentioned cases to be done in the present work make for the first time a climatic design framework for the use of BIPVs in Iran.

### 1.1. The Importance of Using BIPVs

The global cumulative photovoltaic (PV) capacity exceeded half a terawatt in 2019, 580.1 GW of which accounted for grid-tied installations and 3.4 GW for off-grid equipment [3]. It is surmised that most of these facilities are conventional ground-mounted solar farms. However, besides being a pollution-free and renewable energy production source without moving components, PV modules can also be integrated into the building architecture, including the façade [4,5]. PV modules can be used freely as the building envelope or construction material for integration into the architecture, and since electrical system design supports architectural decisions, BIPVs offer excellent performance under ideal conditions or even partial shadow [3]. From a commercial point of view, more than 80% of BIPV systems are roof-mounted, whereas the rest are integrated into the façade [6,7] (Figure 1). Moreover, façade-mounted BIPV devices are less developed [8]. A critical point in installing PVs (including BIPV) on buildings is that the modules must be fully integrated, in both aesthetic and technical terms, to be accepted by the construction industry and the public, and that is particularly true for the façade [9]. All in all, BIPV is a key concept in sustainable architecture and a promising solution for promoting reliance on renewable energies in built environments [10,11].

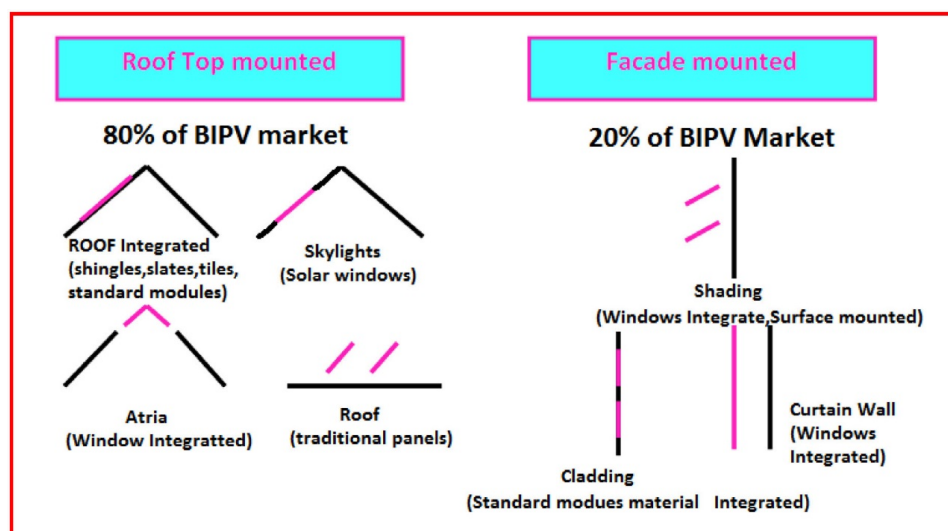


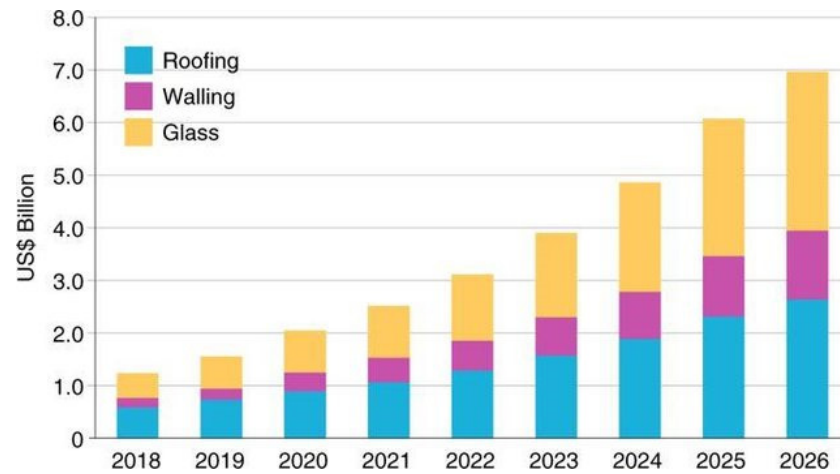
**Figure 1.** BIPV applications in sustainable building [7].

### 1.2. The Latest Status of BIPVs

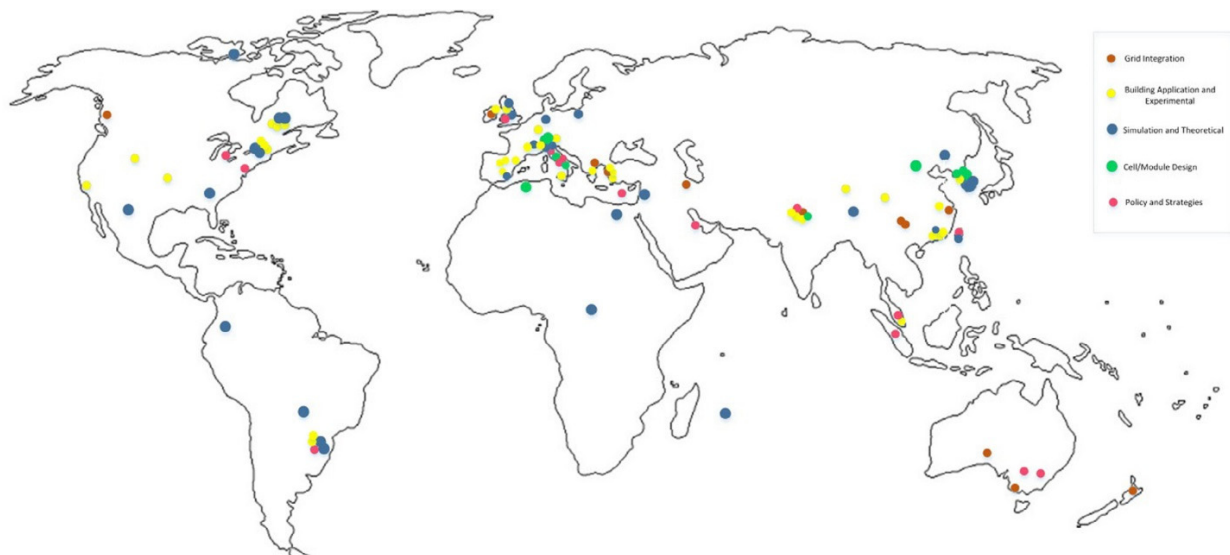
As one of the world's most rapidly expanding industries, BIPV deals with PV cells that are integrated into the building envelope, including the façade and the roof, for clean solar energy production and is a major technology in the field of net-zero energy buildings (NZEB) [12]. A report published on 15 July 2020 [13] on the BIPV industry paints an attractive future of the market in the world. It is estimated that, despite the COVID-19 crisis facing the world, USD 12.7 billion is invested in BIPVs in 2020, which is expected to rise to USD 39.9 billion by 2027, suggesting a 17.8% Compound Annual Growth Rate (CAGR) for the 2020–2027 period. With a 26.91% share of the global industry, the U.S. BIPV market is estimated to be worth USD 3.4 billion. BIPV is a growing international industry with China, the world's second-largest economy, anticipated to invest nearly USD 9.4 billion in the sector in 2020–2027, which corresponds to a 22.8% CAGR. Other notable BIPV markets include Japan and Canada, which are predicted to grow by 12.8 and 15.7% in 2020–2027. Moreover, by 2027, Germany, as a leading country in the sector, is anticipated to attain a 14% CAGR, whereas other EU markets will have invested USD 9.4 billion [13].

Figure 2 shows the projected annual global revenue of the BIPV market between 2018 and 2026. Moreover, according to Figure 3, most previous studies on the network, BIPV systems, and relevant policies before 2017 that focused on the energy, economics,

and environmental analysis were carried out in North America, South Europe, Southeast Asia, and Australia, with little research done in other regions, including Iran, on which the present work focuses.



**Figure 2.** Predicted annual worldwide BIPV commercial market revenue (2018–2026) [14].



**Figure 3.** Studies about the BIPV indicated on the world map according to the study area [15].

Mordor Intelligence’s region-specific prediction of the BIPV market for the 2020–2025 period suggests Australia, Southeast Asia, and Iran, from the Middle East, are leading countries in BIPV system development (Figure 4).

### 1.3. Types of BIPVs

As new BIPV systems are installed, engineers and designers have presented several innovative products, while manufacturers continue supplying the growing market demand [17]. Some major BIPV firms, including Schott, Solar, Sanyo, Sharp, and Sun-tech, work on developing new BIPV products to be used as construction materials, skylights, and windows [18]. Based on performance, materials, and their mechanical and electrical properties, BIPV products are classified into five groups [19,20] (as illustrated in Figure 5).

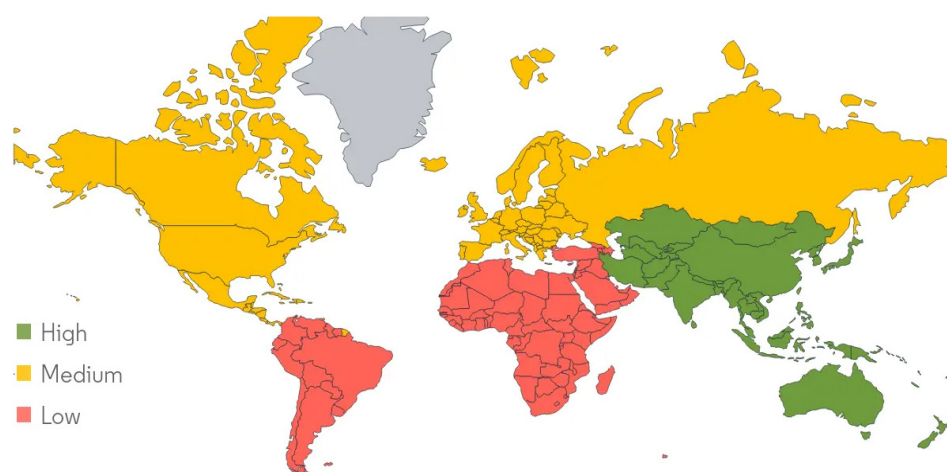


Figure 4. Building-integrated photovoltaics (BIPV) market growth rate by region, 2020–2025 [16].



Figure 5. Classification of BIPV products [21].

Moreover, the new BIPV envelopes protect the interior spaces against the harsh external environment in addition to producing power [22].

1.4. Literature Review

In the following (Table 1), recent works in the study of BIPV systems are reviewed.

Table 1. Literature review for electrifying the BIPV.

Source	Purpose of Study	Analysis and Method Used	Results
[5]	The technical and economic feasibility of using a thin-film cadmium telluride (CdTe) BIPV system in the same building in six Brazilian cities	EnergyPlus and PVSyst	The results showed that the net annual energy consumption of the studied building could be supplied by BIPV systems installed on the roof and the façade.
[23]	Evaluated the technical and economic performance of Italy’s first BIPV project after being in operation for 13 years, predicting the system’s overall performance during its lifetime	Visual inspection And infrared thermography	It was found that the system’s performance did not deteriorate drastically over 13 years. The performance decay was measured at 0.37% per year, which is less than that in a typical multi-crystalline silicon system—around 0.5% per year.
[24]	A life cycle cost analysis (LCCA) for a façade-mounted 127.5 kWp BIPV system with an estimated 55.5 MWh/m <sup>2</sup> power output that was set up in Drammen, Norway.	Mendeley database	The LCCA indicators, namely discounted payback period (DPP), internal rate of return (IRR), cumulative net present value (NPV), and levelized cost of energy (LCOE), were 22 years, 6%, 478,934 NOK, and 1.28 NOK/kWh

Table 1. Cont.

Source	Purpose of Study	Analysis and Method Used	Results
[25]	Evaluation of the economic aspect of BIPV systems as building envelopes with different orientations for implementation in all EU capitals, as well as capitals of Norway and Switzerland.	Economic analysis	As an envelope for the entire building, the BIPV system not only repays all investment costs but also can be a source of revenue for the residents.
[26]	The energy and economic performance of BIPV systems and also other influential factors, including the transmitted solar gain, weather conditions, building orientation, and the type of photovoltaic devices in three Iranian cities, namely Tehran, Bandar Abbas, and Tabriz.	DesignBuilder And EnergyPlus	Energy consumption highly depends on the building's orientation, and the minimum consumption demand in Tehran and Tabriz is achieved on the south side of the BIPV, but on the north side in Bandar Abbas. The maximum energy demand in Tehran was achieved at 285°, but at 60° in Tabriz and 255° in Bandar Abbas.
[27]	BIM-PVSITES toolkit for a technical-economic evaluation of the BIPV system in a cluster of small residential buildings in Ludvika, Sweden	BIM platform (Revit) and PVSITES	Simulation results for the 615 m <sup>2</sup> BIPV, comprising 776 BIPV modules, three solar string-optimizers, and a heat exchanger suggests that the system can produce 35.7 kWp at a maximum rate of 27,394 kWh/year.
[28]	Comparison of the performance of thin-film cadmium telluride (CdTe) BIPV systems installed on a flat roof and east, west, and north sides of the building in a tropical climate in Kuala Pahang, Malaysia	Photovoltaic Geographical Information System (PVGIS)	The results showed the performance ratios for the 7 kW system mounted on the flat roof, 2.3 kW system on the east and west sides, and 5.5 kW system on the north side were 76.26, 70, 70.53, and 66.42%, respectively.

### 1.5. Contribution of Present Work

According to recent studies, it has been observed that so far no study has been done on the impact of different climates on BIPV performance as well as the ranking of different cities in order to find the most suitable climate. Therefore, in the present work, using the output data of HOMER software, the weighting of effective parameters has been done by the SWARA method and then the EDAS method has been used to rank the cities. Finally, ARAS, WASPAS, and TOPSIS techniques are used to validate the results. Given the extent and multiplicity of climates studied, it can be claimed that the results of the present work or the method used to analyze the results can be used for all other parts of the world.

## 2. Studied Cities

Figure 6 shows the location of the studied cities and their climatic conditions. Furthermore, other important information from the cities for simulation, including the monthly average solar radiation, geographical specifications, and the annual average clearness index, is presented in Table 2.

Table 2. Information of cities under study.

City	Monthly Average Solar Radiation (kWh/m <sup>2</sup> —Day)	Longitude (XX° XX' East)	Latitude (XX° XX' North)	Annual Average Clearness Index	Köppen Climate Classification [29]
Dezful	5.51	48 50	32 40	0.646	BSh
Gonbad	5.07	58 59	34 40	0.607	BSk
Jask	6.18	57 50	25 59	0.683	BWh
Marand	4.71	45 59	38 40	0.591	BSk
Ramsar	4.34	50 59	36 59	0.534	Cfa
Shahrekord	5.06	50 59	32 30	0.593	BSk
Tabas	5.17	56 90	33 60	0.609	BWh
Yazd	5.15	54 40	31 59	0.601	BWh

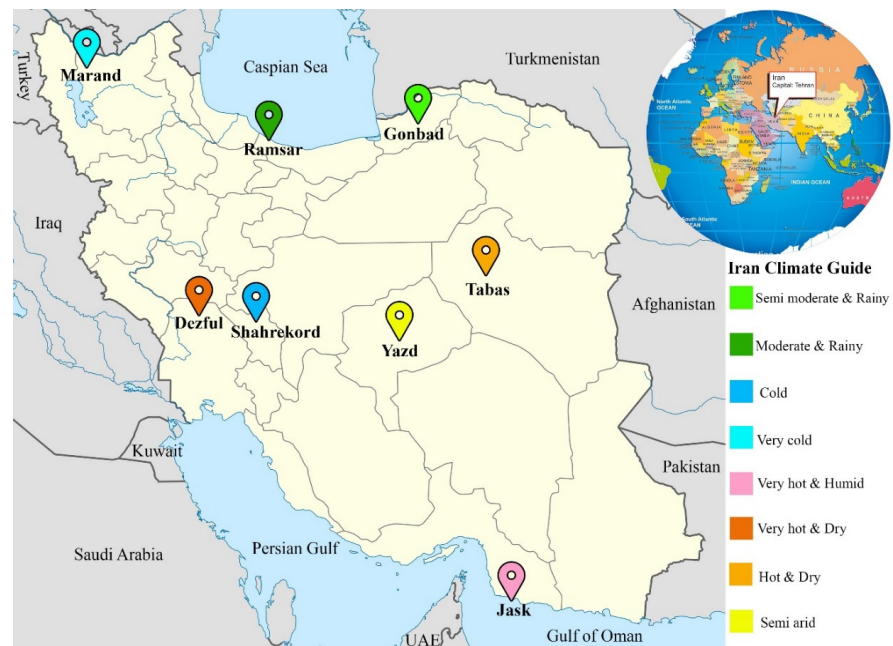


Figure 6. Locations of cities under study.

### 3. Software Used

In this study, simulations were done in HOMER software. HOMER is among the best software for the design of electricity microgrids [30,31] and is used for modeling and optimizing hybrid renewable energy-based systems. Features of HOMER include the feasibility of accurate simulation of the system under study at various time intervals and the possibility of estimating final costs and determining the rate by which the system is optimized [32,33].

The performed simulation flowchart is shown in Figure 7. As can be seen, the data required for the simulation are presented as input to the simulation and optimization sections as well as to the sensitivity analysis.

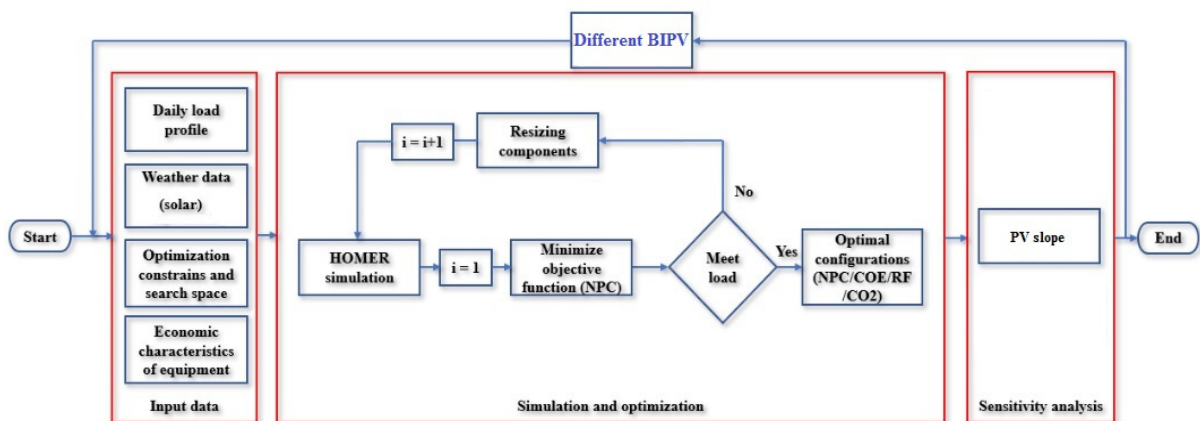


Figure 7. Optimization flowchart for the present work by HOMER software.

### 4. Methodology

#### 4.1. HOMER Software

HOMER software uses the following equations to calculate the amount of electricity generated by photovoltaic cells ( $P_{PV}$ ) [34,35] and to calculate the average air clearness index

$(\overline{k_T})$  [36–38] by taking the average monthly radiation data and the geographical location of the study area:

$$H_{oh} = \frac{24 \times 60}{\pi} G_{sc} \times d_r \times (\omega_s \cdot \sin \varphi \cdot \sin \delta + \cos \varphi \cdot \cos \delta \cdot \sin \omega_s) \quad (1)$$

$$d_r = 1 + 0.033 \cos\left(\frac{2\pi n}{365}\right) \quad (2)$$

$$\delta = 0.409 \sin\left(\frac{2\pi n}{365} - 1.35\right) \quad (3)$$

$$\omega_s = \arccos(-\tan \varphi \cdot \tan \delta) \quad (4)$$

$$\overline{k_T} = \frac{\overline{H}}{H_{oh}} \quad (5)$$

$$P_{pv} = Y_{pv} \times f_{pv} \times \frac{\overline{H_T}}{\overline{H_{T,STC}}} \quad (6)$$

Regarding the performance of HOMER software, different configurations including the lowest total net present cost (NPC) should be ranked in the first place based on the total NPC parameter [39,40]. Economic calculations in HOMER software are performed through the following equations [41–43]:

$$NPC = \frac{C_{ann,total}}{CRF(i, R_{proj})} \quad (7)$$

$$CRF = \frac{i(1+i)^N}{(1+i)^N - 1} \quad (8)$$

$$i = \frac{i' - f}{1 + f} \quad (9)$$

$$COE = \frac{C_{ann,total}}{E_{Load Served}} \quad (10)$$

According to Figures 1 and 5, to investigate the effect of solar cell slope on the generated electricity, four angles of  $0^\circ$ ,  $30^\circ$ ,  $60^\circ$ , and  $90^\circ$  were considered.

If net electricity is calculated on a monthly basis, HOMER software calculates the total annual energy cost through the following equation [44]:

$$C_{grid.energy} = \sum_i^{rates} \sum_j^{12} \begin{cases} E_{net \text{ grid purchases}.i.j} \cdot C_{power.i} & \text{if } E_{net \text{ grid purchases}.i.j} \geq 0 \\ E_{net \text{ grid purchases}.i.j} \cdot C_{sellback.i} & \text{if } E_{net \text{ grid purchases}.i.j} < 0 \end{cases} \quad (11)$$

#### 4.2. SWARA Method

The SWARA method is one of the precise multi-criteria decision-making methods and is used to determine the weight of criteria. It was introduced by Keršulienė et al. in 2010 [45]. One of the distinguishing characteristics of this technique in comparison to similar methods is the precise assessment of the opinions of the experts, considering the consultation of the experts during the process of assessment and less pair comparison than other methods [45–50].

The main steps of this method are as follows [45]:

- First step: the indices are placed in accordance with their importance from the most significant to least significant;
- Second Step: relative significance of each index ( $S_j$ ) is determined.

- Third step: the  $K_j$  coefficient, which is a function that measures the relative significance of each index [45].

$$K_j = S_j + 1 \quad (12)$$

- Fourth step: the initial weight of each index is calculated through equation 13. The weight of the most significant index is considered to be equal to 1 [45].

$$q_j = \frac{q_{j-1}}{K_j} \quad (13)$$

- Fifth Step: the final normal weight is calculated through equation 14 [45].

$$w_j = \frac{q_j}{\sum q_j} \quad (14)$$

#### 4.3. EDAS Technique

The EDAS technique was proposed by Gharabaei et al. in 2015 [51]. In this technique, the distance is not calculated based on the positive or negative ideal. Instead, the desirability of the options is evaluated based on their positive distance from the positive distance from the average (PDA) average and their negative distance from the negative distance from the average (NDA) average [51]. The steps of the EDAS technique are as follows [46,51]:

Step One: the Decision Matrix is created, in which  $X_{ij}$  is the value of option  $i$  in  $j$  criteria, based on Equation (15) [46,51].

$$X = [X_{ij}]_{n \times m} = \begin{bmatrix} X_{11} & X_{12} & \cdots & X_{1m} \\ X_{21} & X_{22} & \cdots & X_{2m} \\ \vdots & \vdots & \vdots & \vdots \\ X_{n1} & X_{n2} & \cdots & X_{nm} \end{bmatrix} \quad (15)$$

Step Two: the average solution of criteria will be obtained on the basis of Equation (16) [46,51].

$$AV_j = \frac{\sum_{i=1}^n X_{ij}}{n} \quad AV = [AV_j]_{1 \times m} \quad (16)$$

Step Three: the value of the PDA and the NDA is calculated through Equations (17) and (18) [46,51].

$$PDA = [PDA_{ij}]_{n \times m} \quad (17)$$

$$NDA = [NDA_{ij}]_{n \times m} \quad (18)$$

If the criterion is a benefit, Equations (19) and (20) will be used [46,51].

$$PDA_{ij} = \frac{\max(0, (X_{ij} - AV_j))}{AV_j} \quad (19)$$

$$NDA_{ij} = \frac{\max(0, (AV_j - X_{ij}))}{AV_j} \quad (20)$$

If the criterion is a cost, Equations (21) and (22) will be used [46,51].

$$PDA_{ij} = \frac{\max(0, (AV_j - X_{ij}))}{AV_j} \quad (21)$$

$$NDA_{ij} = \frac{\max(0, (X_{ij} - AV_j))}{AV_j} \quad (22)$$

Step Four: Equations (23) and (24) are employed to calculate the values of SP and SN [46,51].

$$SP_i = \sum_{j=1}^m w_j PDA_{ij} \quad (23)$$

$$SN_i = \sum_{j=1}^m w_j NDA_{ij} \quad (24)$$

Step Five: the values of SP and SN calculated in the previous step are normalized using Equations (25) and (26) [46,51].

$$NSP_i = \frac{SP_i}{\max_i(SP_i)} \quad (25)$$

$$NSN_i = 1 - \frac{SN_i}{\max_i(SN_i)} \quad (26)$$

Step Six: the final score of the options was calculated using Equation (27) and the options were ranked [46,51].

$$AS_i = \frac{1}{2}(NSP_i + NSN_i) \quad 0 \leq AS_i \leq 1 \quad (27)$$

The options are ranked based on AS values.

#### 4.4. ARAS Technique

The ARAS method is one of the multi-criteria decision-making (MCDM) methods that is used to rank the options [51]. The steps of the Aras method are as follows [52]:

First, the decision matrix  $m \times n$  is formed, where m represents the number of options and n represents the number of criteria. Then, the optimal value of the j criterion is determined as follows [52]:

$$\begin{aligned} x_{0j} &= \max_i x_{ij}, & \text{if } \max_i x_{ij} & \text{is preferable} \\ x_{0j} &= \min_i x_{ij}^*, & \text{if } \min_i x_{ij}^* & \text{is preferable} \end{aligned} \quad (28)$$

The decision matrix must then be normalized to compare the values of the options. Normalization of criteria is done in two ways:

For profit criteria, normalization is done as follows [52]:

$$\bar{x}_{ij} = \frac{x_{ij}}{\sum_{i=0}^m x_{ij}} \quad (29)$$

For cost criteria, normalization is done as follows [52]:

$$x_{ij} = \frac{1}{x_{ij}^*} \quad \bar{x}_{ij} = \frac{x_{ij}}{\sum_{i=0}^m x_{ij}} \quad (30)$$

The weights are then applied in the matrix to obtain the matrix  $\hat{X}$ . The weights given must meet the following conditions [52]:

$$0 < w_j < 1$$

$$\sum_{j=1}^n w_j = 1 \quad (31)$$

$$\hat{X} = \begin{bmatrix} \hat{x}_{01} & \dots & \hat{x}_{0j} & \dots & \hat{x}_{0n} \\ \vdots & \ddots & \vdots & \ddots & \vdots \\ \hat{x}_{i1} & \dots & \hat{x}_{ij} & \dots & \hat{x}_{in} \\ \vdots & \ddots & \vdots & \ddots & \vdots \\ \hat{x}_{m1} & \dots & \hat{x}_{mj} & \dots & \hat{x}_{mn} \end{bmatrix} \quad i = \overline{0, m}; \quad j = \overline{1, n} \quad (32)$$

$$\hat{x}_{ij} = \bar{x}_{ij} \times w_j; \quad i = \overline{0, m} \quad (33)$$

where  $w_j$  is the importance of the criterion  $j$  and  $\bar{x}_{ij}$  is the normalized value of the criterion  $j$ .

Next, the optimality function must be calculated, which is calculated according to the following equation [52]:

$$S_i = \sum_{j=1}^n \hat{x}_{ij}; \quad i = \overline{0, m} \quad (34)$$

where  $S_i$  is the optimal function value for option  $i$ .

Finally, the degree of utility is calculated for each option [52]:

$$K_i = \frac{S_i}{S_0}; \quad i = \overline{0, m} \quad (35)$$

Options are ranked based on  $K_i$  values.

#### 4.5. WASPAS Technique

The WASPAS method is one of the MCDM techniques for ranking that is useful in complex decision issues and its output is very accurate. The steps of the WASPAS method are as follows [53]:

First, the decision matrix  $m \times n$  is formed, where  $m$  represents the number of options and  $n$  represents the number of criteria. Then, the optimal value of the  $j$  criterion is determined as follows [53]:

$$\begin{aligned} x_{0j} &= \max_i x_{ij}, & \text{if } \max_i x_{ij} & \text{is preferable} \\ x_{0j} &= \min_i x_{ij}^*, & \text{if } \min_i x_{ij}^* & \text{is preferable} \end{aligned} \quad (36)$$

The decision matrix must then be normalized to compare the values of the options. Normalization of criteria is done in two ways:

For profit criteria, normalization is done as follows [53]:

$$\bar{x}_{ij} = \frac{x_{ij}}{\max_i x_{ij}} \quad (37)$$

For cost criteria, normalization is done as follows [53]:

$$x_{ij} = \frac{\min_i x_{ij}}{x_{ij}^*} \quad (38)$$

The normalized decision matrix for the WSM model is then calculated using the following equation [53]:

$$\hat{x}_q = \begin{bmatrix} \hat{x}_{11} & \dots & \hat{x}_{1j} & \dots & \hat{x}_{1n} \\ \vdots & \ddots & \vdots & \ddots & \vdots \\ \hat{x}_{i1} & \dots & \hat{x}_{ij} & \dots & \hat{x}_{in} \\ \vdots & \ddots & \vdots & \ddots & \vdots \\ \hat{x}_{m1} & \dots & \hat{x}_{mj} & \dots & \hat{x}_{mn} \end{bmatrix}; \hat{x}_{ij} = \bar{x}_{ij} w_j, \quad i = \overline{1, m}; \quad j = \overline{1, n} \quad (39)$$

The normalized decision matrix for the WPM model is then calculated using the following equation [53]:

$$\bar{X}_p = \begin{bmatrix} \bar{x}_{11} & \dots & \bar{x}_{1j} & \dots & \bar{x}_{1n} \\ \vdots & \ddots & \vdots & \ddots & \vdots \\ \bar{x}_{i1} & \dots & \bar{x}_{ij} & \dots & \bar{x}_{in} \\ \vdots & \ddots & \vdots & \ddots & \vdots \\ \bar{x}_{m1} & \dots & \bar{x}_{mj} & \dots & \bar{x}_{mn} \end{bmatrix}; \bar{x}_{ij} = \bar{x}_{ij}^{w_j}, i = \overline{1, m}; j = \overline{1, n} \quad (40)$$

According to the WSM model in the WASPAS method,  $Q_i$  is calculated for each option [53]:

$$Q_i = \sum_{j=1}^n \hat{x}_{ij}, i = \overline{1, m} \quad (41)$$

According to the WPM model,  $P_i$  is calculated for each option [53]:

$$P_i = \sum_{j=1}^n \bar{x}_{ij}, i = \overline{1, m} \quad (42)$$

The value of  $WPS_i$  is calculated according to the steps of the WASPAS method and the options are ranked accordingly [53]:

$$WPS_i = 0.5 \sum_{j=1}^m Q_i + 0.5 \sum_{j=1}^m P_i \quad (43)$$

#### 4.6. TOPSIS Technique

TOPSIS is a compensatory multiple attribute decision-making (MADM) method, which involves measuring the distance between each alternative and the ideal and anti-ideal alternatives. The steps of TOPSIS method are as follows [54]:

In this method, the values of the criteria must first be normalized. The following equation is used to normalize the criteria [54]:

$$r_{ij} = \frac{x_{ij}}{\sqrt{\sum_{i=1}^M x_{ij}^2}} \quad (44)$$

The next step is to form the normalized decision matrix  $V$  based on the set of weights  $W = (w_1, w_2, \dots, w_n)$  [54]:

$$v_{ij} = w_{ij} r_{ij} \quad (45)$$

Then, the ideal alternative ( $A^*$ ) and the anti-ideal alternative ( $A^-$ ) are determined using Equations (46) and (47) [54]:

$$A^* = \{(\max v_{ij} | j \in J), (\min v_{ij} | j \in J') | i = 1, 2, 3, \dots, M\} = \{v_{1^*}, v_{2^*}, \dots, v_{N^*}\} \quad (46)$$

$$A^- = \{(\min v_{ij} | j \in J), (\max v_{ij} | j \in J') | i = 1, 2, 3, \dots, M\} = \{v_{1^-}, v_{2^-}, \dots, v_{N^-}\} \quad (47)$$

Next, the Euclidean distance of alternative  $j$  from the ideal and anti-ideal alternatives is obtained using Equations (48) and (49) [54]:

$$S_i^* = \sqrt{\sum_{j=1}^n (v_{ij} - v_j^*)^2}, i = 1, \dots, M \quad (48)$$

$$S_i^- = \sqrt{\sum_{j=1}^n (v_{ij} - v_j^-)^2}, i = 1, \dots, M \quad (49)$$

The relative closeness of alternative  $A_j$  to the ideal alternative is then calculated by Equation (50) [54]:

$$C_{i^*} = \frac{S_{i^-}}{S_{i^*} + S_{i^-}}, \quad 0 \leq C_{i^*} \leq 1, \quad i = 1, 2, 3, \dots, M \tag{50}$$

Finally, the alternatives are ranked based on their  $C_i$ .

### 5. Input Data

Climate data on solar radiation, which is an average of 20 years [55–57], has been extracted from the NASA site. The schematic of the simulation performed in the present work is shown in Figure 8. As can be seen from Figure 8, the BIPV building under study has the possibility of exchanging electricity with the national electricity grid, which converts the direct current (DC) electricity generated by solar cells to the alternative current (AC) power consumed by an electric converter. The advantage of connecting the BIPV building under study to the grid power is reducing the cost of the photovoltaic system by selling the surplus electricity to the grid.

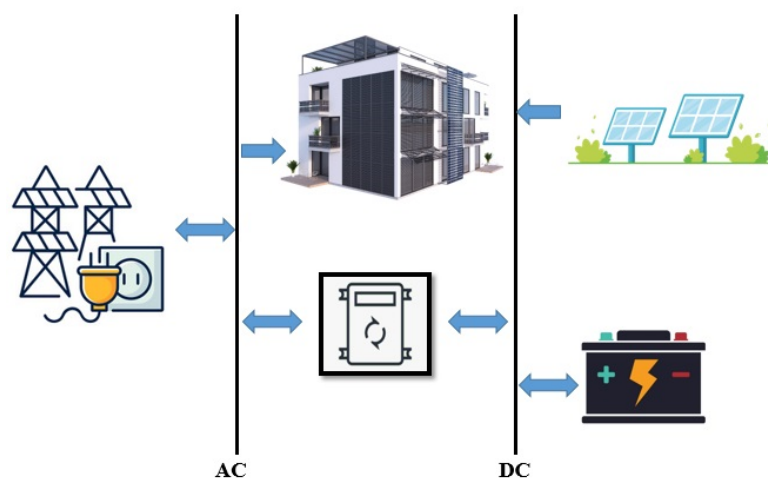


Figure 8. Schematic of the simulated system.

Required data include power consumption profile (Figure 9), constraints, and search space (Table 3), as well as prices and characteristics of equipment used (Table 3). According to Figure 9, it can be seen that the maximum electrical load required in different months is from 18 p.m to 22 p.m. The average annual load is 21 kWh/day with a peak value of 2.7 kW. Other software inputs in the present work are annual interest rate of 18% [58,59], a project lifetime of 25 years [60,61], and emission fines equal to zero [62,63]. Moreover, the electricity exchange prices with the national electricity grid in three off-peak times (23 p.m to 8 a.m), normal times (8 a.m to 16 p.m), and peak times (16 p.m to 23 p.m) are equal to 0.05, 0.07 and 0.12 USD/kWh [64], respectively.

Table 3. Information of BIPV system under study.

Equipment	Cost			Size (kW)	Other Information
	Capital (\$)	Replacement (\$)	Operating & Maintenance (\$/Year)		
PV [65]	1000	1000	5	0, 50	Lifetime: 25 years Ground reflectance: 20%

Table 3. Cont.

Equipment	Cost			Size (kW)	Other Information
	Capital (\$)	Replacement (\$)	Operating & Maintenance (\$/Year)		
Battery T-105 [66]	174	174	5	0–5	Nominal Voltage: 6 Nominal capacity: 225Ah
Converter [67]	200	200	10	0–20	Lifetime: 10 years Efficiency: 90%

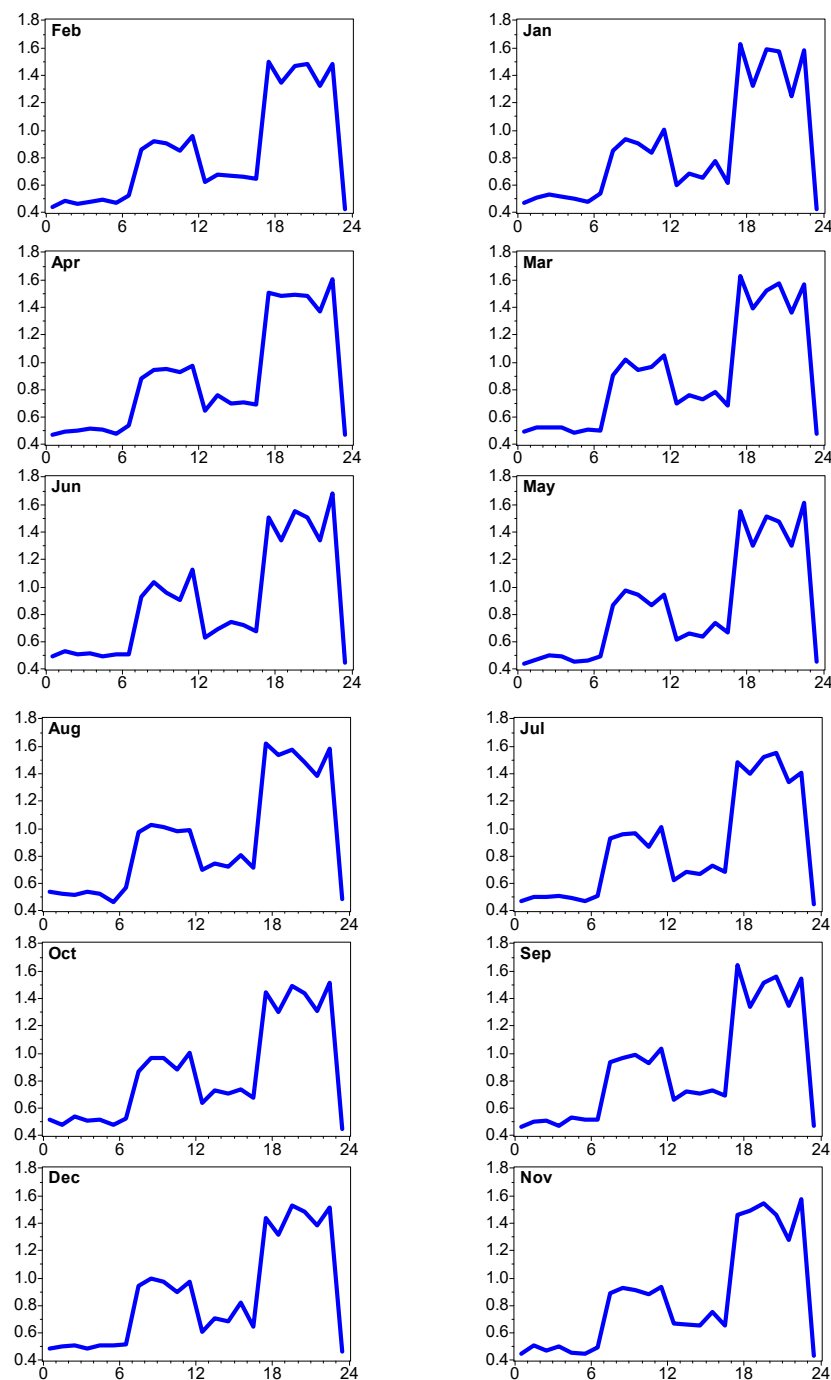


Figure 9. Profile of average required electric load in kW over a year.

## 6. Results

### 6.1. HOMER Simulation

The results of the simulations performed for different installation angles of solar cells, each of which represents a type of BIPV structure, are given in Tables 4–7. The results show that the most economically appropriate angle is 30°, followed by 0°, 60°, and 90°. The lowest cost of electricity generated at 0.073 USD/kWh is related to the 30° angle and Jask city. In this case, about 89% of electricity is generated by solar cells, which leads to the shortest return on investment between the angles and cities under study with 11.7 years. At the top economic city and the optimal angle, about 39 MWh of electricity is generated annually, about 1.5 MWh of excess electricity is generated annually, and the annual emission of about 16.5 tons of CO<sub>2</sub> pollutants is prevented. Of course, it should be noted that for Jask city and 30° angle, due to high solar power generation, losses in electrical converters are also maximum.

**Table 4.** Results of slope 0°.

City	Total NPC (\$)	LCOE (\$/kWh)	Renewable Fraction (%)	Payback Time (Year)	PV Production (kWh/Year)	Excess Electricity (kWh/Year)	PV Capacity Factor (%)	Inverter Losses (kWh/Year)	Net Sold to Grid (kWh/Year)	CO <sub>2</sub> Emission Avoided (kg/Year)
Dezful	16,543	0.096	87.1	13.6	32,147	1703	18.3	3045	19,772	12,496
Gonbad	17,660	0.111	85.4	15.5	29,566	2025	16.9	2754	17,159	10,845
Jask	15,767	0.082	88.2	12.5	36,050	1383	20.6	3144	23,572	14,897
Marand	17,768	0.119	85.1	15.7	27,476	1606	15.7	2587	15,655	9894
Ramsar	18,627	0.136	83.3	17.8	25,319	2182	14.5	2314	13,195	8339
Shahrekord	17,461	0.108	86	15	29,524	1395	16.9	2813	17,688	11,179
Tabas	17,401	0.106	86.1	14.9	30,162	1294	17.2	2887	18,353	11,599
Yazd	17,413	0.106	86.1	14.9	30,049	1370	17.2	2868	18,182	11,491

**Table 5.** Results of slope 30°.

City	Total NPC (\$)	LCOE (\$/kWh)	Renewable Fraction (%)	Payback Time (Year)	PV Production (kWh/Year)	Excess Electricity (kWh/Year)	PV Capacity Factor (%)	Inverter Losses (kWh/Year)	Net Sold to Grid (kWh/Year)	CO <sub>2</sub> Emission Avoided (kg/Year)
Dezful	15,696	0.081	88.4	12.4	35,757	1114	20.4	3465	23,550	14,884
Gonbad	16,858	0.094	86.9	13.9	33,445	1706	19.1	3174	20,936	13,232
Jask	15,108	0.073	88.8	11.7	39,014	1496	22.3	3752	26,138	16,519
Marand	16,790	0.098	86.9	13.8	31,808	1466	18.2	3034	19,680	12,438
Ramsar	18,024	0.117	85	16	28,449	1827	16.2	2662	16,331	10,321
Shahrekord	16,892	0.097	86.9	14	32,218	1533	18.4	3069	19,987	12,632
Tabas	16,617	0.092	87.2	13.6	33,802	1732	19.3	3207	21,234	13,420
Yazd	16,776	0.094	87	13.8	33,064	1626	18.9	3144	20,665	13,061

**Table 6.** Results of slope 60°.

City	Total NPC (\$)	LCOE (\$/kWh)	Renewable Fraction (%)	Payback Time (Year)	PV Production (kWh/Year)	Excess Electricity (kWh/Year)	PV Capacity Factor (%)	Inverter Losses (kWh/Year)	Net Sold to Grid (kWh/Year)	CO <sub>2</sub> Emission Avoided (kg/Year)
Dezful	16,866	0.1	86.5	14.1	31,984	2260	18.3	2973	19,123	12,085
Gonbad	17,731	0.108	85.4	15.5	30,629	2208	17.5	2842	17,950	11,345
Jask	16,688	0.092	87	13.7	33,788	1670	19.3	3212	21,278	13,448
Marand	17,472	0.11	85.6	15	29,789	2116	17	2768	17,278	10,919
Ramsar	18,731	0.133	83.3	17.8	26,068	2222	14.9	2385	13,833	8743
Shahrekord	17,957	0.119	84.6	16.1	28,515	2481	16.3	2604	15,801	9987
Tabas	17,605	0.108	85.6	15.2	30,599	2146	17.5	2846	17,980	11,363
Yazd	17,852	0.112	85.2	15.7	29,440	1855	16.8	2759	17,198	10,869

**Table 7.** Results of slope 90°.

City	Total NPC (\$)	LCOE (\$/kWh)	Renewable Fraction (%)	Payback Time (Year)	PV Production (kwh/Year)	Excess Electricity (kWh/Year)	PV Capacity Factor (%)	Inverter Losses (kWh/Year)	Net Sold to Grid (kWh/Year)	CO <sub>2</sub> Emission Avoided (kg/Year)
Dezful	19,470	0.161	80.8	22	22,228	2362	12.7	1986	10,251	6479
Gonbad	19,858	0.165	80.1	23.5	22,053	2440	12.6	1961	10,023	6335
Jask	19,603	0.160	80.8	22.5	22,420	2269	12.8	2015	10,508	6641
Marand	19,503	0.163	80.5	22.2	22,092	2538	12.6	1955	9970	6301
Ramsar	20,389	0.193	77.4	n/a	19,110	2493	10.9	1662	7327	4631
Shahrekord	20,154	0.186	78.2	24.8	19,768	2508	11.3	1726	7905	4996
Tabas	19,829	0.166	80.1	23.4	21,763	2320	12.4	1944	9871	6238
Yazd	20,068	0.180	78.6	24.5	20,539	2768	11.7	1777	8366	5287

Regarding the results, it should be noted that the most economically unsuitable city among the cities under study is Ramsar, which for an angle of 90° has the highest cost per kWh of electricity generated, which is equal to USD 0.193. For this case, the lowest percentage of renewable energy, 77.4%, has been obtained. For Ramsar and 90° angles, the payback time is more than 25 years of the project’s lifetime. The lowest capacity factor for solar cells is 10.9%, and the lowest level of CO<sub>2</sub> emission prevention is 4.6 tons per year for this condition.

6.2. Data Analysis

6.2.1. Criteria Weighting Using SWARA Method

To assess the significance of the criteria in the SWARA method, the opinions of eight academic professional experts and activists in the field of renewable energies, with more than eight years of experience, were used to weight the criteria in the SWARA method. In accordance with the steps of the SWARA method, the decision-makers ranked the data with respect to their significance after consultation and reaching a consensus. Then, the significance of the criteria was determined based on the questionnaire completed by the experts, and, in accordance with the SWARA method, the weight of the criteria was calculated; the results are included in Table 8.

LCOE (USD/kWh), payback time (year), and total NPC (USD) criteria with weights of 0.159, 0.150, and 0.134 had the highest significance among the criteria. The weights are compared in Figure 10. Based on the results of Figure 10, it is clear that the lowest weights are inverter losses, excess electricity, and renewable fraction, respectively, and their normalized weights are 0.045, 0.056 and 0.067, respectively.

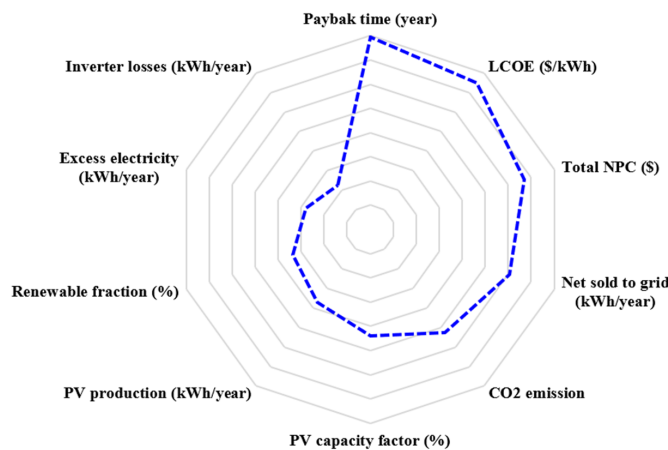


**Figure 10.** Comparing the criteria weights.

**Table 8.** Calculating the weight of indices of technical and financial characteristics.

Criteria	Average Relative Importance	Calculation of $K_j$	Calculation of the Initial Weight	Calculation of the Final Normalized Weight
Payback time (year)	1	1	1	0.159
LCOE (\$/kWh)	0.06	1.06	0.943	0.150
Total NPC (\$)	0.12	1.12	0.842	0.134
Net sold to grid (kWh/year)	0.11	1.11	0.759	0.121
CO <sub>2</sub> emission	0.15	1.15	0.660	0.105
PV capacity factor (%)	0.19	1.19	0.555	0.088
PV production (kWh/year)	0.19	1.19	0.466	0.074
Renewable fraction (%)	0.11	1.11	0.420	0.067
Excess electricity (kWh/year)	0.19	1.19	0.353	0.056
Inverter losses (kWh/year)	0.25	1.25	0.282	0.045

### 6.2.2. Ranking Cities of Iran Using MCDM Methods

In this section, the cities in Iran were ranked in slopes with angles of 0°, 30°, 60°, and 90° using the EDAS technique. Then, ARAS, WASPAS, and TOPSIS techniques were employed to validate the results.

At first, the decision-making matrix was created for ranking the cities on a 0° slope. The results are provided in Table 9.

Afterward, the EDAS technique was used to rank the identified cities; then, the results were validated using ARAS, WASPAS, and TOPSIS techniques. The final results of ranking the cities are provided in Table 10.

The results of ranking revealed that in all four techniques, the cities of Jask, Dezful, and Gonbad were all selected as the most suitable cities on a 0° slope. The results of the ranking are compared in Figure 11. Based on the results in Figure 11, for the 0° angle, all four ranking methods have exactly the same results. Ramsar, Marand, and Shahrekord are the cities that are more unsuitable, respectively.

The decision-making matrix was created to rank the cities on a 30° slope. The results are provided in Table 11.

Then, the identified cities were ranked using the EDAS technique; then, the results were validated using ARAS, WASPAS, and TOPSIS techniques. The final results of ranking the cities are provided in Table 12.

**Table 9.** The 0° slope decision-making matrix.

City	Total NPC (\$)	LCOE (\$/kWh)	Renewable Fraction (%)	Payback Time (Year)	PV Production (kWh/Year)	Excess Electricity (kWh/Year)	PV Capacity Factor (%)	Inverter Losses (kWh/Year)	Net Sold to Grid (kWh/Year)	CO <sub>2</sub> Emission Avoided (kg/Year)
Dezful	16,543	0.096	87.1	13.6	32,147	1703	18.3	3045	19,772	12,496
Gonbad	17,660	0.111	85.4	15.5	29,566	2025	16.9	2754	17,159	10,845

Table 9. Cont.

City	Total NPC (\$)	LCOE (\$/kWh)	Renewable Fraction (%)	Payback Time (Year)	PV Production (kWh/Year)	Excess Electricity (kWh/Year)	PV Capacity Factor (%)	Inverter Losses (kWh/Year)	Net Sold to Grid (kWh/Year)	CO <sub>2</sub> Emission Avoided (kg/Year)
Jask	15,767	0.082	88.2	12.5	36,050	1383	20.6	3144	23,572	14,897
Marand	17,768	0.119	85.1	15.7	27,476	1606	15.7	2587	15,655	9894
Ramsar	18,627	0.136	83.3	17.8	25,319	2182	14.5	2314	13,195	8339
Shahrekord	17,461	0.108	86	15	29,524	1395	16.9	2813	17,688	11,179
Tabas	17,401	0.106	86.1	14.9	30,162	1294	17.2	2887	18,353	11,599
Yazd	17,413	0.106	86.1	14.9	30,049	1370	17.2	2868	18,182	11,491

Table 10. Results of ranking of cities on a 0° slope.

City	EDAS		ARAS		WASPAS		TOPSIS	
	AS <sub>i</sub>	Rank	K <sub>i</sub>	Rank	WPS <sub>i</sub>	Rank	C <sub>i</sub>	Rank
Dezful	0.712	2	0.869	2	0.871	2	0.654	2
Gonbad	0.524	3	0.817	3	0.817	3	0.466	3
Jask	0.921	1	0.937	1	0.935	1	0.743	1
Marand	0.302	7	0.761	7	0.764	7	0.302	7
Ramsar	0.161	8	0.739	8	0.734	8	0.276	8
Shahrekord	0.422	6	0.790	6	0.793	6	0.433	6
Tabas	0.437	5	0.794	5	0.796	5	0.460	5
Yazd	0.451	4	0.797	4	0.800	4	0.462	4

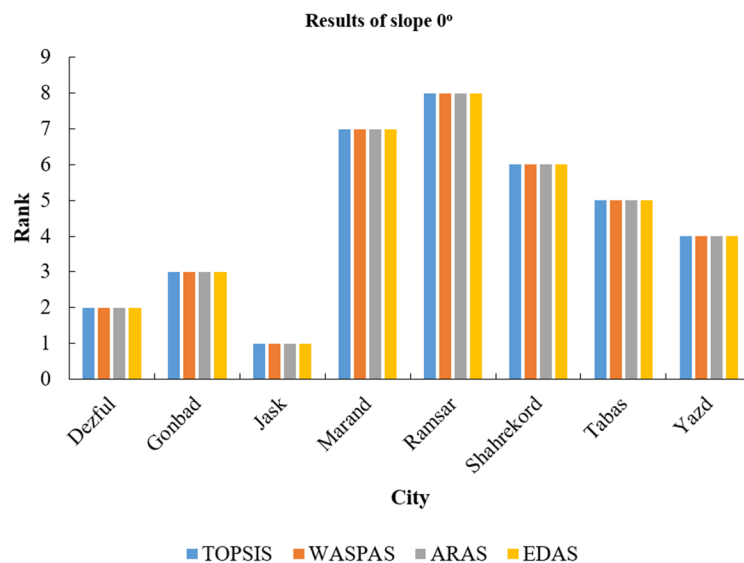


Figure 11. Comparing the ranking of cities on a 0° slope.

**Table 11.** The 30° slope decision-making matrix.

City	Total NPC (\$)	LCOE (\$/kWh)	Renewable Fraction (%)	Payback Time (Year)	PV Production (kWh/Year)	Excess Electricity (kWh/Year)	PV Capacity Factor (kW)	Inverter Losses (kWh/Year)	Net Sold to Grid (kWh/Year)	CO <sub>2</sub> Emission Avoided (kg/Year)
Dezful	15,696	0.081	88.4	12.4	35,757	1114	20.4	3465	23,550	14,884
Gonbad	16,858	0.094	86.9	13.9	33,445	1706	19.1	3174	20,936	13,232
Jask	15,108	0.073	88.8	11.7	39,014	1496	22.3	3752	26,138	16,519
Marand	16,790	0.098	86.9	13.8	31,808	1466	18.2	3034	19,680	12,438
Ramsar	18,024	0.117	85	16	28,449	1827	16.2	2662	16,331	10,321
Shahrekord	16,892	0.097	86.9	14	32,218	1533	18.4	3069	19,987	12,632
Tabas	16,617	0.092	87.2	13.6	33,802	1732	19.3	3207	21,234	13,420
Yazd	16,776	0.094	87	13.8	33,064	1626	18.9	3144	20,665	13,061

**Table 12.** Results of ranking of cities on a 30° slope.

City	EDAS		ARAS		WASPAS		TOPSIS	
	AS <sub>i</sub>	Rank	K <sub>i</sub>	Rank	WPS <sub>i</sub>	Rank	C <sub>i</sub>	Rank
Dezful	0.702	2	0.901	2	0.900	2	0.708	2
Gonbad	0.492	4	0.844	4	0.846	4	0.503	4
Jask	0.966	1	0.977	1	0.975	1	0.864	1
Marand	0.386	7	0.817	7	0.819	7	0.411	7
Ramsar	0.056	8	0.742	8	0.742	8	0.196	8
Shahrekord	0.404	6	0.821	6	0.823	6	0.426	6
Tabas	0.539	3	0.856	3	0.858	3	0.545	3
Yazd	0.475	5	0.840	5	0.841	5	0.491	5

The results of ranking indicated that on a 30° slope the cities of Jask, Dezful, and Tabas were all selected as the most suitable cities using all four techniques. The results of the ranking are compared in Figure 12. The point from Figure 12 is that the ranking results for a 30° angle are quite similar to a 0° angle.

The decision-making matrix was created to rank the cities on a 60° slope. The results are provided in Table 13.

Then, the identified cities were ranked using the EDAS technique; then, the results were validated using ARAS, WASPAS, and TOPSIS techniques. The final results of ranking the cities are provided in Table 14.

The results of ranking indicated that on a 60° slope the cities of Jask, Dezful, and Tabas were all selected as the most suitable cities in all four techniques. The results of the ranking are compared in Figure 13. An interesting point that can be seen from Figure 13 is that for a 60° angle, the first and second ranks (Jask and Dezful) are the same as the 0° and 30° angles, but the third-most suitable city is Tabas (instead of Gonbad).

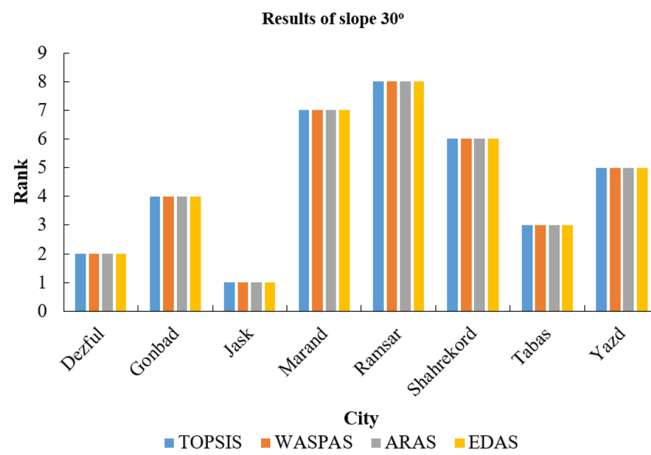


Figure 12. Comparing the ranking of cities on a 30° slope.

Table 13. The 60° slope decision-making matrix.

City	Total NPC (\$)	LCOE (\$/kWh)	Renewable Fraction (%)	Payback Time (Year)	PV Production (kWh/Year)	Excess Electricity (kWh/Year)	PV Capacity Factor (kW)	Inverter Losses (kWh/Year)	Net Sold to Grid (kWh/Year)	CO <sub>2</sub> Emission Avoided (kg/Year)
Dezful	16,866	0.1	86.5	14.1	31,984	2260	18.3	2973	19,123	12,085
Gonbad	17,731	0.108	85.4	15.5	30,629	2208	17.5	2842	17,950	11,345
Jask	16,688	0.092	87	13.7	33,788	1670	19.3	3212	21,278	13,448
Marand	17,472	0.11	85.6	15	29,789	2116	17	2768	17,278	10,919
Ramsar	18,731	0.133	83.3	17.8	26,068	2222	14.9	2385	13,833	8743
Shahrekord	17,957	0.119	84.6	16.1	28,515	2481	16.3	2604	15,801	9987
Tabas	17,605	0.108	85.6	15.2	30,599	2146	17.5	2846	17,980	11,363
Yazd	17,852	0.112	85.2	15.7	29,440	1855	16.8	2759	17,198	10,869

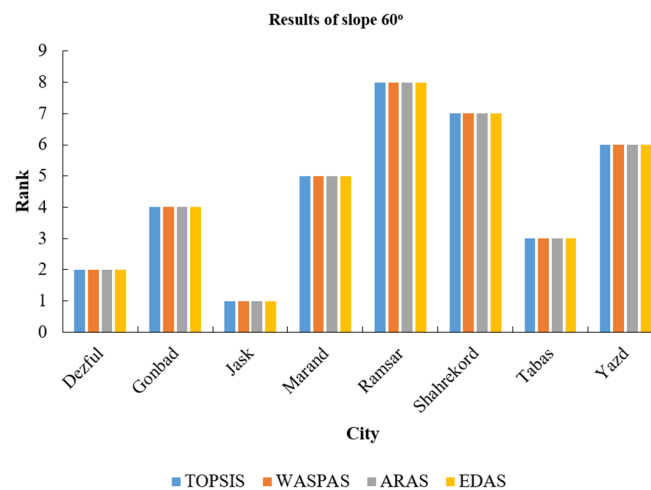


Figure 13. Comparing the ranking of cities on a 60° slope.

**Table 14.** Results of ranking of cities on a 60° slope.

City	EDAS		ARAS		WASPAS		TOPSIS	
	AS <sub>i</sub>	Rank	K <sub>i</sub>	Rank	WPS <sub>i</sub>	Rank	C <sub>i</sub>	Rank
Dezful	0.777	2	0.935	2	0.936	2	0.758	2
Gonbad	0.546	4	0.884	4	0.886	4	0.574	4
Jask	0.932	1	0.969	1	0.967	1	0.803	1
Marand	0.506	5	0.876	5	0.877	5	0.534	5
Ramsar	0.040	8	0.774	8	0.774	8	0.160	8
Shahrekord	0.356	7	0.841	7	0.842	7	0.367	7
Tabas	0.557	3	0.887	3	0.888	3	0.585	3
Yazd	0.418	6	0.856	6	0.857	6	0.469	6

The decision-making matrix was created to rank the cities on a 90° slope; the results are provided in Table 15.

**Table 15.** The 90° slope decision-making matrix.

City	Total NPC (\$)	LCOE (\$/kWh)	Renewable Fraction (%)	Payback Time (Year)	PV Production (kWh/Year)	Excess Electricity (kWh/Year)	PV Capacity Factor (kW)	Inverter Losses (kWh/Year)	Net Sold to Grid (kWh/Year)	CO <sub>2</sub> Emission Avoided (kg/Year)
Dezful	19,470	0.161	80.8	22	22,228	2362	12.7	1986	10,251	6479
Gonbad	19,858	0.165	80.1	23.5	22,053	2440	12.6	1961	10,023	6335
Jask	19,603	0.160	80.8	22.5	22,420	2269	12.8	2015	10,508	6641
Marand	19,503	0.163	80.5	22.2	22,092	2538	12.6	1955	9970	6301
Ramsar	20,389	0.193	77.4	n/a	19,110	2493	10.9	1662	7327	4631
Shahrekord	20,154	0.186	78.2	24.8	19,768	2508	11.3	1726	7905	4996
Tabas	19,829	0.166	80.1	23.4	21,763	2320	12.4	1944	9871	6238
Yazd	20,068	0.180	78.6	24.5	20,539	2768	11.7	1777	8366	5287

Then, the identified cities were ranked using the EDAS technique; then, the results were validated using ARAS, WASPAS, and TOPSIS techniques. The final results of ranking the cities are provided in Table 16.

The results demonstrated that when using EDAS, ARAS, and WASPAS techniques, the most suitable cities are Jask, Dezful, and Marand, respectively. In the TOPSIS technique Dezful, Jask, and Marand were selected as the most suitable cities on a 90° slope, respectively. The results of the ranking are compared in Figure 14. According to Figure 14, it should be noted that unlike the 0°, 30°, and 60° angles, where all four methods showed the same results for ranking, there is a difference between the TOPSIS method and other methods in the 90° angle for selecting the top city.

**Table 16.** Results of ranking of cities on a 90° slope.

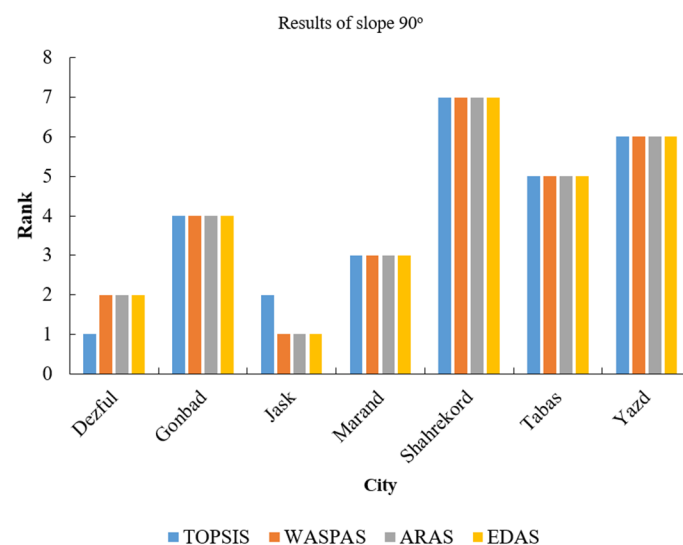
City	EDAS		ARAS		WASPAS		TOPSIS	
	AS <sub>i</sub>	Rank	K <sub>i</sub>	Rank	WPS <sub>i</sub>	Rank	C <sub>i</sub>	Rank
Dezful	0.930	2	0.977	2	0.978	2	0.809	1
Gonbad	0.686	4	0.956	4	0.957	4	0.7171	4
Jask	0.958	1	0.978	1	0.978	1	0.797	2
Marand	0.839	3	0.971	3	0.971	3	0.791	3
Ramsar	–	–	–	–	–	–	–	–
Shahrekord	0.062	7	0.873	7	0.872	7	0.136	7
Tabas	0.599	5	0.948	5	0.949	5	0.672	5
Yazd	0.266	6	0.899	6	0.898	6	0.268	6

The average rank of cities on a 90° slope revealed that the cities of Jask, Dezful, and Marand are the most suitable on a 90° slope, respectively. The results are provided in Table 17.

The results of ranking with EDAS, ARAS, WASPAS, and TOPSIS techniques and on slopes of 0°, 30°, 60°, and 90° indicated that the city of Jask is the most suitable place.

**Table 17.** Final ranking of cities on a 90° slope.

City	EDAS	ARAS	WASPAS	TOPSIS	Average Ranking	Rank
Dezful	2	2	2	1	1.75	2
Gonbad	4	4	4	4	4	4
Jask	1	1	1	2	1.25	1
Marand	3	3	3	3	3	3
Ramsar	–	–	–	–	–	–
Shahrekord	7	7	7	7	7	7
Tabas	5	5	5	5	5	5
Yazd	6	6	6	6	6	6

**Figure 14.** Comparing the ranking of cities on a 90° slope.

## 7. Conclusions

The construction sector in each country accounts for a large share of energy consumption. Therefore, the use of clean, free, and inexhaustible solar energy in meeting all or part of the needs of buildings seems necessary in Iran. Despite having an extremely high radiation potential, a comprehensive technical–economic–environmental energy study of various types of BIPV in different climates has not been conducted. Therefore, in the present work for the first time, the relevant analyses have been performed using HOMER 2.81 software and the weighting of the effective output parameters of the HOMER 2.81 software has been done by the SWARA method. Then, different cities were ranked using EDAS. The results were also verified by ARAS, WASPAS, and TOPSIS methods. The main results of the present work are as follows:

- 30° and 90° angles were the most suitable and unsuitable angles in terms of economic and solar power generation, respectively.
- The lowest cost per kWh of solar power generated is USD 0.073 (30° angle and Jask city).
- The highest percentage of electricity supply by solar cells is 88.8% (30° angle and Jask city).
- Weighting the parameters of the problem was done using the SWARA method and then the ranking was done using methods EDAS, ARAS, WASPAS, and TOPSIS.
- The results of different ranking methods EDAS, ARAS, and WASPAS were similar, and only the results of the TOPSIS method were different for the cities of Dezful and Jask.
- With normalized weight of 0.159, the “payback time” parameter had the highest weight among the studied parameters. The lowest weight with the amount of 0.045 is related to “inverter losses”.
- In the final ranking of cities, Jask is the most suitable and Ramsar is the most unsuitable.
- For an angle of 30° at Jask city, 39 MWh of solar electricity is generated annually, which prevents the annual emission of 16.5 tons of CO<sub>2</sub> pollutants.
- The lowest return time with 11.7 years is related to Jask city (30° angle), and the highest return time with more than 25 years is related to Ramsar city (90° angle).

**Author Contributions:** Conceptualization, M.J. and Y.Y.; methodology, M.J., S.J.H.D. and S.S.H.D.; software, M.J. and S.M.F.V.; validation, S.J.H.D. and S.S.H.D.; formal analysis, S.J.H.D. and S.S.H.D. and S.M.F.V.; investigation, Y.Y.; resources, Y.Y.; data curation, I.P.; writing—original draft preparation, M.J., Y.Y., S.J.H.D. and S.S.H.D.; writing—review and editing, M.J. and S.J.H.D.; visualization, I.P. and S.M.F.V.; supervision, M.J.; project administration, M.J. All authors have read and agreed to the published version of the manuscript.

**Funding:** This research received no external funding.

**Data Availability Statement:** All data used to support the findings of this study are included within the article.

**Conflicts of Interest:** The authors declare no conflict of interest.

## References

1. Martín-Chivelet, N.; Kapsis, K.; Wilson, H.R.; Delisle, V.; Yang, R.; Olivier, L.; Polo, J.; Eisenlohr, J.; Roy, B.; Maturi, L.; et al. Building-Integrated Photovoltaic (BIPV) products and systems: A review of energy-related behavior. *Energy Build.* **2022**, *262*, 111998. [CrossRef]
2. Skandalos, N.; Wang, M.; Kapsalis, V.; D’Agostino, D.; Parker, D.; Bhuvad, S.S.; Peng, J.; Karamanis, D. Building PV integration according to regional climate conditions: BIPV regional adaptability extending Köppen-Geiger climate classification against urban and climate-related temperature increases. *Renew. Sustain. Energy Rev.* **2022**, *169*, 112950. [CrossRef]
3. IRENA. *Renewable Capacity Statistics 2020*; International Renewable Energy Agency: Abu Dhabi, UAE, 2020; Available online: <https://irena.org/publications/2020/Mar/Renewable-Capacity-Statistics-2020> (accessed on 20 June 2021).
4. Mints, P. The Solar Flare–SPV Market Research. 2019. Available online: <https://www.spvmarketresearch.com> (accessed on 20 June 2021).

5. Sorgato, M.J.; Schneider, K.; R  ther, R. Technical and economic evaluation of thin-film CdTe building-integrated photovoltaics (BIPV) replacing fa ade and rooftop materials in office buildings in a warm and sunny climate. *Renew. Energ.* **2018**, *118*, 84–98. [CrossRef]
6. Shukla, A.K.; Sudhakar, K.; Baredar, P. Recent advancement in BIPV product technologies: A review. *Energy Build.* **2017**, *140*, 188–195. [CrossRef]
7. Krawietz, A.; Silke, A. Sustainable buildings and BIPV: An international perspective. SETA Network. 2011. Available online: [https://www.bre.co.uk/filelibrary/BIPV%202/Silke\\_Krawietz.pdf](https://www.bre.co.uk/filelibrary/BIPV%202/Silke_Krawietz.pdf) (accessed on 20 June 2021).
8. Saretta, E.; Caputo, P.; Frontini, F. A review study about energy renovation of building facades with BIPV in urban environment. *Sustain. Cities Soc.* **2019**, *44*, 343–355. [CrossRef]
9. Kuhn, T.E.; Erban, C.; Heinrich, M.; Eisenlohr, J.; Ensslen, F.; Neuhaus, D.H. Review of Technological Design Options for Building Integrated Photovoltaics (BIPV). *Energy Build.* **2020**, *23*, 110381. [CrossRef]
10. Gon alves, J.E.; van Hooff, T.; Saelens, D. Understanding the behaviour of naturally-ventilated BIPV modules: A sensitivity analysis. *Renew. Energ.* **2020**, *161*, 133–148. [CrossRef]
11. Goncalves, J.E.; van Hooff, T.; Saelens, D. A physics-based high-resolution BIPV model for building performance simulations. *Sol. Energy* **2020**, *204*, 585–599. [CrossRef]
12. Gholami, H.; R stvik, H.N.; M ller-Eie, D. Holistic economic analysis of building integrated photovoltaics (BIPV) system: Case studies evaluation. *Energy Build.* **2019**, *203*, 109461. [CrossRef]
13. ReportLinker. Global Building Integrated Photovoltaics (BiPV) Industry. 2021. Available online: [https://www.reportlinker.com/p03037269/Global-Building-Integrated-Photovoltaics-BIPV-Industry.html?utm\\_source=GNW](https://www.reportlinker.com/p03037269/Global-Building-Integrated-Photovoltaics-BIPV-Industry.html?utm_source=GNW) (accessed on 20 June 2021).
14. Ballif, C.; Perret-Aebi, L.E.; Lufkin, S.; Rey, E. Integrated thinking for photovoltaics in buildings. *Nat. Energy* **2018**, *3*, 438–442. [CrossRef]
15. Biyik, E.; Araz, M.; Hepbasli, A.; Shahrestani, M.; Yao, R.; Shao, L.; Essah, E.; Oliveira, A.C.; Del Cano, T.; Rico, E.; et al. A key review of building integrated photovoltaic (BIPV) systems. *Eng. Sci. Technol. Int. J.* **2017**, *20*, 833–858. [CrossRef]
16. Mordor Intelligence. Building Integrated Photovoltaic (BIPV) Market–Growth, Trends, COVID-19 Impact, and Forecasts (2021–2026). 2020. Available online: <https://www.mordorintelligence.com/industry-reports/building-integrated-photovoltaic-market> (accessed on 20 June 2021).
17. Posnansky, M.; Szacsny, T.; Eckmanns, A.; J rgens, J. New electricity construction materials for roofs and fa ades. *Renew. Energy* **1998**, *15*, 541–544. [CrossRef]
18. Benemann, J.; Chehab, O.; Schaar-Gabriel, E. Building-integrated PV modules. *Sol. Energy Mater. Sol. Cells* **2001**, *67*, 345–354. [CrossRef]
19. Fraile, D.; Despotou, E.; Latour, M.; Slusaz, T.; Weiss, I.; Caneva, S.; Helm, P.; Goodal, J.; Fintikakis, N.; Schellekens, E. PV Diffusion in the Building Sector, European Photovoltaic Industry Association, Sunrise Project. 2008. Available online: <https://www.eupvsec-proceedings.com/proceedings?paper=2654> (accessed on 20 June 2021).
20. Shukla, A.K.; Sudhakar, K.; Baredar, P. Exergetic assessment of BIPV module using parametric and photonic energy methods: A review. *Energy Build.* **2016**, *119*, 62–73. [CrossRef]
21. Shukla, A.K.; Sudhakar, K.; Baredar, P. A comprehensive review on design of building integrated photovoltaic system. *Energy Build.* **2016**, *128*, 99–110. [CrossRef]
22. Roy, A.; Ghosh, A.; Bhandari, S.; Sundaram, S.; Mallick, T.K. Perovskite solar cells for BIPV application: A review. *Buildings* **2020**, *10*, 129. [CrossRef]
23. Aste, N.; Del Pero, C.; Leonforte, F. The first Italian BIPV project: Case study and long-term performance analysis. *Sol. Energy* **2016**, *134*, 340–352. [CrossRef]
24. Gholami, H.; R stvik, H.N.; Kumar, N.M.; Chopra, S.S. Lifecycle cost analysis (LCCA) of tailor-made building integrated photovoltaics (BIPV) fa ade: Solsmaragden case study in Norway. *Sol. Energy* **2020**, *211*, 488–502. [CrossRef]
25. Gholami, H.; R stvik, H.N. Economic analysis of BIPV systems as a building envelope material for building skins in Europe. *Energy* **2020**, *204*, 117931. [CrossRef]
26. Fazelpour, F.; Ziasistani, N.; Nazari, P.; Nazari, P.; Ziasistani, N. Techno-Economic Assessment of BIPV Systems in Three Cities of Iran. *Multidiscip. Digit. Publ. Inst. Proc.* **2018**, *2*, 1474.
27. Quintana, S.; Huang, P.; Saini, P.; Zhang, X. A preliminary techno-economic study of a building integrated photovoltaic (BIPV) system for a residential building cluster in Sweden by the integrated toolkit of BIM and PVSITES. *Intell. Build. Int.* **2021**, *13*, 51–69. [CrossRef]
28. Kumar, N.M.; Sudhakar, K.; Samykano, M. Performance evaluation of CdTe BIPV roof and fa ades in tropical weather conditions. *Energy Sources A Recovery Util. Environ. Eff.* **2020**, *42*, 1057–1071. [CrossRef]
29. Mazzeo, D.; Matera, N.; De Luca, P.; Baglivo, C.; Congedo, P.M.; Oliveti, G. A literature review and statistical analysis of photovoltaic-wind hybrid renewable system research by considering the most relevant 550 articles: An upgradable matrix literature database. *J. Clean. Prod.* **2021**, *295*, 126070. [CrossRef]
30. Alturki, A.A. Optimal design for a hybrid microgrid-hydrogen storage facility in Saudi Arabia. *Energy Sustain. Soc.* **2020**, *12*, 1–17. [CrossRef]

31. Elmorshedy, M.F.; Elkadeem, M.R.; Kotb, K.M.; Taha, I.B.; El-Nemr, M.K.; Kandeal, A.W.; Sharshir, S.W.; Almakhles, D.J.; Imam, S.M. Feasibility study and performance analysis of microgrid with 100% hybrid renewables for a real gricultural irrigation application. *Sustain. Energy Technol. Assess.* **2022**, *53*, 102746. [[CrossRef](#)]
32. Wei, Y.; Han, T.; Wang, S.; Qin, Y.; Lu, L.; Han, X.; Ouyang, M. An efficient data-driven optimal sizing framework for photovoltaics-battery-based electric vehicle charging microgrid. *J. Energy Storage* **2022**, *55*, 105670. [[CrossRef](#)]
33. Ariae, A.R.; Jahangiri, M.; Fakhri, M.H.; Shamsabadi, A.A. Simulation of Biogas Utilization Effect on the Economic Efficiency and Greenhouse Gas Emission: A Case Study in Isfahan, Iran. *Int. J. Renew. Energy Dev.* **2019**, *8*, 149–160. [[CrossRef](#)]
34. Dehkordi, M.H.R.; Isfahani, A.H.M.; Rasti, E.; Nosouhi, R.; Akbari, M.; Jahangiri, M. Energy-Economic-Environmental assessment of solar-wind-biomass systems for finding the best areas in Iran: A case study using GIS maps. *Sustain. Energy Technol. Assess.* **2022**, *53*, 102652. [[CrossRef](#)]
35. Jahangiri, M.; Khalili Geshnigani, M.; Beigi Kheradmand, A.; Riahi, R. Meeting the Hospital Oxygen Demand with a Decentralized Autonomous PV System: Effect of PV Tracking Systems. *Iran. J. Sci. Technol. Trans. Electr. Eng.* **2022**, *47*, 1–15. [[CrossRef](#)]
36. Mostafaeipour, A.; Jahangiri, M.; Saghaei, H.; Raiesi Goojani, A.; Chowdhury, M.; Techato, K. Impact of Different Solar Trackers on Hydrogen Production: A Case Study in Iran. *Int. J. Photoenergy* **2022**, *2022*, 3186287. [[CrossRef](#)]
37. Rezaei, M.; Khalilpour, K.R.; Jahangiri, M. Multi-criteria location identification for wind/solar based hydrogen generation: The case of capital cities of a developing country. *Int. J. Hydrog. Energy* **2020**, *45*, 33151–33168. [[CrossRef](#)]
38. Jahangiri, M.; Raeiszadeh, F.; Alayi, R.; Najafi, A.; Tahmasebi, A. Development of Rural Tourism in Iran Using PV-Based System: Finding the Best Economic Configuration. *J. Renew. Energy Environ.* **2022**, 1–9.
39. Ampah, J.D.; Afrane, S.; Agyekum, E.B.; Adun, H.; Yusuf, A.A.; Bamisile, O. Electric vehicles development in Sub-Saharan Africa: Performance assessment of a standalone renewable energy systems for hydrogen refuelling and electricity charging stations (HRECS). *J. Clean. Prod.* **2022**, *376*, 134238. [[CrossRef](#)]
40. Agyekum, E.B.; Ampah, J.D.; Afrane, S.; Adebayo, T.S.; Agbozo, E. A 3E, hydrogen production, irrigation, and employment potential assessment of a hybrid energy system for tropical weather conditions—Combination of HOMER software, shannon entropy, and TOPSIS. *Int. J. Hydrog. Energy* **2022**, *47*, 31073–31097. [[CrossRef](#)]
41. Al Garni, H.Z.; Mas’ud, A.A.; Baseer, M.A.; Ramli, M.A. Techno-economic optimization and sensitivity analysis of a PV/Wind/diesel/battery system in Saudi Arabia using a combined dispatch strategy. *Sustain. Energy Technol. Assess.* **2022**, *53*, 102730. [[CrossRef](#)]
42. Ampah, J.D.; Jin, C.; Agyekum, E.B.; Afrane, S.; Geng, Z.; Adun, H.; Yusuf, A.A.; Liu, H.; Bamisile, O. Performance analysis and socio-enviro-economic feasibility study of a new hybrid energy system-based decarbonization approach for coal mine sites. *Sci. Total Environ.* **2022**, *854*, 158820. [[CrossRef](#)]
43. Dehghan, H.; Pourfayaz, F.; Shahsavari, A. Multicriteria decision and Geographic Information System-based locational analysis and techno-economic assessment of a hybrid energy system. *Renew. Energy* **2022**, *198*, 189–199. [[CrossRef](#)]
44. Mostafaeipour, A.; Rezaei, M.; Jahangiri, M.; Qolipour, M. Feasibility analysis of a new tree-shaped wind turbine for urban application: A case study. *Energy Environ.* **2020**, *31*, 1230–1256. [[CrossRef](#)]
45. Keršulienė, V.; Zavadskas, E.K.; Turskis, Z. Selection of rational dispute resolution method by applying new step-wise weight assessment ratio analysis (SWARA). *J. Bus. Econ. Manag.* **2010**, *11*, 243–258. [[CrossRef](#)]
46. Mostafaeipour, A.; Dehshiri, S.J.H.; Dehshiri, S.S.H.; Jahangiri, M. Prioritization of potential locations for harnessing wind energy to produce hydrogen in Afghanistan. *Int. J. Hydrog. Energy* **2020**, *45*, 33169–33184. [[CrossRef](#)]
47. Mostafaeipour, A.; Jahangiri, M.; Haghani, A.; Dehshiri, S.J.H.; Dehshiri, S.S.H.; Sedaghat, A.; Saghaei, H.; Akinlabi, E.T.; Sichilalu, S.M.; Chowdhury, M.S.; et al. Statistical evaluation of using the new generation of wind turbines in South Africa. *Energy Rep.* **2020**, *6*, 2816–2827. [[CrossRef](#)]
48. Mostafaeipour, A.; Dehshiri, S.J.H.; Dehshiri, S.S.H. Ranking locations for producing hydrogen using geothermal energy in Afghanistan. *Int. J. Hydrog. Energy* **2020**, *45*, 15924–15940. [[CrossRef](#)]
49. Dahooie, J.H.; Dehshiri, S.J.H.; Banaitis, A.; Binkytė-Vėlienė, A. Identifying and prioritizing cost reduction solutions in the supply chain by integrating value engineering and gray multi-criteria decision-making. *Technol. Econ. Dev. Econ.* **2020**, *26*, 1311–1338. [[CrossRef](#)]
50. Mostafaeipour, A.; Hosseini Dehshiri, S.J.; Hosseini Dehshiri, S.S.; Jahangiri, M.; Techato, K. A thorough analysis of potential geothermal project locations in Afghanistan. *Sustainability* **2020**, *12*, 8397. [[CrossRef](#)]
51. Keshavarz Ghorabae, M.; Zavadskas, E.K.; Olfat, L.; Turskis, Z. Multi-criteria inventory classification using a new method of evaluation based on distance from average solution (EDAS). *Informatica* **2015**, *26*, 435–451. [[CrossRef](#)]
52. Zavadskas, E.K.; Turskis, Z. A new additive ratio assessment (ARAS) method in multicriteria decision making. *Technol. Econ. Dev. Econ.* **2010**, *16*, 159–172. [[CrossRef](#)]
53. Zavadskas, E.K.; Turskis, Z.; Antucheviciene, J.; Zakarevicius, A. Optimization of weighted aggregated sum product assessment. *Elektron. Ir Elektrotech.* **2012**, *122*, 3–6. [[CrossRef](#)]
54. Hwang, C.L.; Yoon, K. Methods for multiple attribute decision making. In *Multiple Attribute Decision Making*; Springer: Berlin/Heidelberg, Germany, 1981; pp. 58–191.
55. Sharma, R.; Murthy, S.S.; Dutta, P.; Rao, B.S. Performance of solid state hydrogen storage assisted standalone polygeneration microgrids for various climatic zones of India. *Energy* **2022**, *258*, 124869. [[CrossRef](#)]

56. Miah, M.A.; Rakib, N.; Habib, M.A.; Hasanuzzaman, M.; Saha, S. Techno-economic analysis and environmental impact assessment of 3 MW photovoltaic power plant in Bangladesh: A case study based on real data. *Environ. Dev. Sustain.* **2022**, *141*, 1–19. [[CrossRef](#)]
57. Kuetche, C.F.M.; Tsuanyo, D.; Fopah-Lele, A. Analysis of Hybrid Energy Systems for Telecommunications Equipment: A Case Study in Buea Cameroon. *Proc. E3S Web Conf. EDP Sci.* **2022**, *354*, 02007. [[CrossRef](#)]
58. Shabestari, S.T.; Kasaeian, A.; Rad, M.A.V.; Fard, H.F.; Yan, W.M.; Pourfayaz, F. Techno-financial evaluation of a hybrid renewable solution for supplying the predicted power outages by machine learning methods in rural areas. *Renew. Energy* **2022**, *194*, 1303–1325. [[CrossRef](#)]
59. Mostafaeipour, A.; Qolipour, M.; Rezaei, M.; Jahangiri, M.; Goli, A.; Sedaghat, A. A novel integrated approach for ranking solar energy location planning: A case study. *J. Eng. Des. Technol.* **2020**, *19*, 698–720.
60. Mostafaeipour, A.; Sedaghat, A.; Hedayatpour, M.; Jahangiri, M. Location planning for production of bioethanol fuel from agricultural residues in the south of Caspian Sea. *Environ. Dev.* **2020**, *33*, 100500. [[CrossRef](#)]
61. Riayatsyah, T.M.I.; Geumpana, T.A.; Fattah, I.M.; Mahlia, T.M. Techno-Economic Analysis of Hybrid Diesel Generators and Renewable Energy for a Remote Island in the Indian Ocean Using HOMER Pro. *Sustainability* **2022**, *14*, 9846. [[CrossRef](#)]
62. Kamal, M.M.; Asharaf, I.; Fernandez, E. Optimal renewable integrated rural energy planning for sustainable energy development. *Sustain. Energy Technol. Assess.* **2022**, *53*, 102581.
63. Zaniyani, J.R.; Dehkordi, R.H.; Bibak, A.; Bayat, P.; Jahangiri, M. Examining the possibility of using solar energy to provide warm water using RETScreen4 software (Case study: Nasr primary school of pibalut). *Curr. World Environ.* **2015**, *10*, 835. [[CrossRef](#)]
64. Akhavan Shams, S.; Ahmadi, R. Dynamic optimization of solar-wind hybrid system connected to electrical battery or hydrogen as an energy storage system. *Int. J. Energy Res.* **2021**, *45*, 10630–10654. [[CrossRef](#)]
65. Rezk, H.; Alghassab, M.; Ziedan, H.A. An optimal sizing of stand-alone hybrid PV-fuel cell-battery to desalinate seawater at saudi NEOM city. *Processes* **2020**, *8*, 382. [[CrossRef](#)]
66. Jahangiri, M.; Haghani, A.; Heidarian, S.; Mostafaeipour, A.; Raiesi, H.A.; Shamsabadi, A.A. Sensitivity analysis of using solar cells in regional electricity power supply of off-grid power systems in Iran. *J. Eng. Des. Technol.* **2020**, *18*, 1849–1866. [[CrossRef](#)]
67. Ibrahim, M.M.; Mostafa, N.H.; Osman, A.H.; Hesham, A. Performance analysis of a stand-alone hybrid energy system for desalination unit in Egypt. *Energy Convers. Manag.* **2020**, *215*, 112941. [[CrossRef](#)]

**Disclaimer/Publisher’s Note:** The statements, opinions and data contained in all publications are solely those of the individual author(s) and contributor(s) and not of MDPI and/or the editor(s). MDPI and/or the editor(s) disclaim responsibility for any injury to people or property resulting from any ideas, methods, instructions or products referred to in the content.